



Acceleration-selective arterial spin labeling MR angiography for visualization of brain arteriovenous malformations

Osamu Togao¹ · Akio Hiwatashi² · Koji Yamashita¹ · Daichi Momosaka¹ · Makoto Obara³ · Ataru Nishimura⁴ · Koichi Arimura⁴ · Nobuhiro Hata⁴ · Koji Iihara⁴ · Marc Van Cauteren³ · Hiroshi Honda¹

Received: 11 February 2019 / Accepted: 11 April 2019 / Published online: 23 April 2019
© Springer-Verlag GmbH Germany, part of Springer Nature 2019

Abstract

Purpose To evaluate the performance of acceleration-selective arterial spin labeling (AccASL) MR angiography in the visualization of brain arteriovenous malformations (AVMs) in comparison with digital subtraction angiography (DSA) and time-of-flight (TOF) MR angiography.

Methods Twenty-one patients with brain AVM (mean age 31.1 ± 18.6 years; 11 males, 10 females) underwent TOF and AccASL MR angiography and DSA. Two neuroradiologists conducted an observer study for detection, nidus size, eloquence, venous drainage pattern, and Spetzler-Martin (SM) grade. The evaluations included the visualization of each AVM component with reference to DSA and assessments of contrast-to-noise ratio (CNR). The kappa statistic, repeated measures analysis of variance, Wilcoxon matched pairs test, and paired *t* test were used.

Results Both observers detected more AVMs with AccASL (95.2%, 90.5% for Observers 1 and 2) than with TOF (76.2% and 71.4%, respectively). The inter-modality agreement between AccASL and DSA was almost perfect for the eloquence, venous drainage pattern, and SM grade for Observer 1 and moderate for the venous drainage pattern and substantial for the eloquence and SM grade for Observer 2. The visualization scores were higher with AccASL than with TOF for the feeding artery (AccASL, 4.5 ± 1.0 vs. TOF, 3.9 ± 1.5 , $p = 0.0214$), nidus (4.6 ± 1.1 vs. 3.2 ± 1.5 , $p = 0.0006$), and draining vein (4.6 ± 1.0 vs. 2.2 ± 1.1 , $p < 0.0001$), respectively. The CNRs in the nidus were higher in AccASL than in TOF (29.9 ± 16.7 vs. 20.8 ± 16.5 , $p = 0.0002$), as in the draining vein (23.2 ± 13.0 vs. 12.6 ± 12.0 , $p = 0.0010$), respectively.

Conclusions AccASL better visualized brain AVMs compared with TOF and was useful for grading without the use of contrast agents.

Keywords Magnetic resonance imaging · Magnetic resonance angiography · Brain · Arteriovenous malformations · Acceleration-selective arterial spin labeling

Introduction

Arteriovenous malformation (AVM) of the brain is a vascular disorder that can cause serious intracranial hemorrhage, with an annual rate of rupture of 2–3% [1, 2]. The bleeding has high morbidity and mortality, with an approx. 42% risk of permanent neurological deficit or death from a hemorrhagic event [3]. Clinically, the Spetzler-Martin (SM) grading system has been used as a method of estimating the risk of intraoperative mortality and morbidity to guide treatment recommendations, based on the size of the nidus, the eloquence of the brain area, and the presence of deep venous drainage. The detection and accurate grading of AVM are necessary to prevent future hemorrhages, reduce intraoperative complications, and ensure better clinical outcomes of patients. Thus, effective vascular

✉ Osamu Togao
togao@radiol.med.kyushu-u.ac.jp

¹ Department of Clinical Radiology, Graduate School of Medical Sciences, Kyushu University, 3-1-1 Maidashi Higashi-ku, Fukuoka 812-8582, Japan

² Department of Molecular Imaging & Diagnosis, Graduate School of Medical Sciences, Kyushu University, 3-1-1 Maidashi Higashi-ku, Fukuoka 812-8582, Japan

³ Philips Japan, 13-37, Kohnan 2-chome, Minato-ku, Tokyo 108-8507, Japan

⁴ Department of Neurosurgery, Graduate School of Medical Sciences, Kyushu University, 3-1-1 Maidashi Higashi-ku, Fukuoka 812-8582, Japan

imaging methods with high diagnostic performance are desirable for optimal medical care.

Digital subtraction angiography (DSA) is the current reference standard for the diagnosis, treatment planning, and post-treatment monitoring of brain AVMs. However, DSA is an invasive procedure which carries the risk of neurological complications and adverse reactions associated with contrast agents. Three-dimensional (3D) time-of-flight (TOF) MR angiography (hereafter “TOF”) is the most common approach for intracranial MR angiography without contrast agent injection, and it has been widely used in clinical practice for evaluations of various vascular lesions [4–6]. Vessel visualization in TOF depends on the inflow effect of unsaturated blood spins into an imaging slab in the inferior-to-superior direction. This setup is thus not optimal for visualizing blood flow that is not in this direction or for slow or complex flow where blood spins remain longer in the imaging slab and are saturated by successive radiofrequency (RF) pulses. Consequently, TOF frequently fails to depict brain AVMs where the blood flow is complex or not in the inferior-to-superior direction.

In 2014, the acceleration-selective arterial spin labeling (AccASL) method was proposed for vascular [7] and perfusion imaging [8]. AccASL uses motion-sensitized gradients (MSGs) in which the effective gradient waveform is such that the first moment (m_1) is zero. This gradient rephases the signal of spins moving at constant velocity, whereas the signal from spins that are subjected to acceleration will be dephased. Since the pulsatile arterial flow has an acceleration component, arterial blood spins will be visualized after subtraction of the labeled images from the non-labeled images. AccASL was adopted to intracranial MR angiography [9], and its clinical application for moyamoya disease was recently reported [10]. Since AccASL MR angiography (hereafter “AccASL”) does not depend on the inflow effect, it may be able to visualize complex or slow flows in brain AVMs.

We conducted the present study to evaluate the performance of AccASL in the visualization of brain AVMs by a comparison with DSA as a reference standard and with conventional TOF.

Materials and methods

This retrospective study was approved by the Institutional Review Board of Kyushu University Hospital, and the requirement for informed consent was waived. Two authors (M.O., M.V.C.) were employees of Philips Healthcare and provided technical support in sequence development but were not involved in the study design or interpretation of the data. The institutional authors, who were not employees of Philips Healthcare, were in control of all the data.

Patients

AccASL has been a part of our routine MR imaging protocol for brain AVM since October 2014. The inclusion criteria for this study are outlined in Fig. 1. The inclusion criteria were (1) patients with brain AVM in whom definite diagnoses were made by the previous DSA and (2) patients who were suspected to have brain AVM. We analyzed the MR imaging data of the 58 consecutive patients who were identified between October 2014 and August 2017. The exclusion criteria were (1) DSA had not been performed ($n = 27$), (2) DSA and MR angiography had not been performed within an interval of 6 months ($n = 10$), (3) DSA revealed no AVMs ($n = 0$), (4) a hemorrhage had occurred within the interval between MR angiography and DSA ($n = 0$), and (5) severe motion artifact was observed on MR angiography ($n = 0$).

A total of 21 patients (11 males and 10 females; mean age 31.1 ± 18.6 years; median age 28 years; age range, 9–63 years) were identified based on the above criteria. The patients' characteristics are summarized in Table 1.

MR angiography

The MR angiography imaging was performed using a 3-T scanner (Ingenia 3.0CX, Philips Healthcare, Best, The Netherlands). The details of the imaging parameters are summarized in Table 2. Figure 2 describes the improved version of AccASL [11]. In this version, two additional 180° refocusing pulses were used in the control module to efficiently suppress spin dispersion and flow voids in major arterial trunks. In the label module, MSGs were applied for a 20-ms period with acceleration encoding such that an acceleration of 1.47 m/s^2 results in a phase accumulation of exactly π . In the control module, no MSGs were applied. MR angiography is obtained by subtracting the images acquired in labeling from those in the control. The TOF was obtained using geometry, spatial resolution ($0.39 \times 0.77 \times 1.00 \text{ mm}$), and scan time (6 min and 9 s) identical to those used for the AccASL.

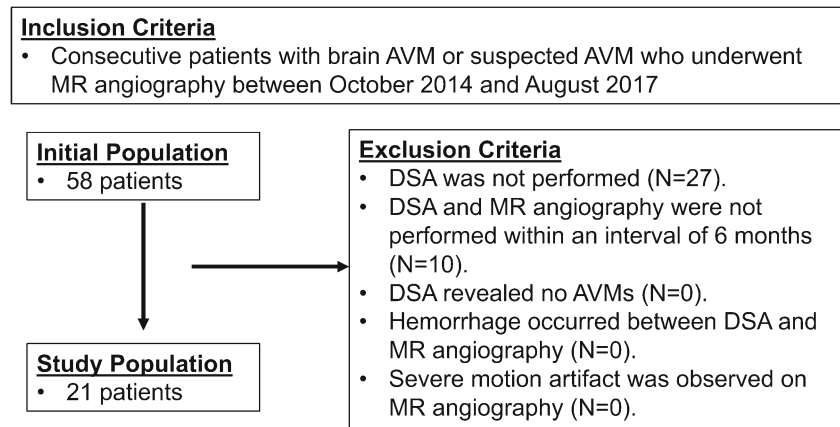
DSA

DSA was performed with a standard protocol on a biplane system (Siemens, Erlangen, Germany). Frontal and lateral views were obtained after the injection of a 4–12-mL bolus of iodinated contrast agent at 2–6 mL/s in each internal carotid artery and vertebral artery.

Image evaluation

Observer study

Two neuroradiologists who were blinded to each patient's clinical information and images including a board-certified

Fig. 1 Patient inclusion and exclusion criteria

radiologist with 15 years of experience (K.Y., Observer 1) and a resident with 4 years of experience in neuroradiology (D.M., Observer 2) participated in the observer test. Neither observer

participated in the case selection. Both observers took part in two reading sessions ≥ 1 month apart. Each session was comprised of half TOF and half AccASL images in a random

Table 1 Clinical data and DSA findings

Patient no./age/gender	Location	Major clinical symptom	Previous hemorrhage (ago)	Nidus size (mm)	Eloquence	Venous drainage pattern	SM grade	Interval between DSA and MRI
1/9/F	Lt. frontal	Dyspnea due to pulmonary AVM	None	19	N	D	2	1 day
2/11/M	Lt. parietal	Weakness of rt. lower limb, headache	19 days	18	E	S/D	3	0 day
3/11/M	Rt. temporal	None	3 years	20	N	S	1	1 day
4/12/F	Lt. frontal	Disturbance of consciousness	21 days	12	N	S	1	16 days
5/12/F	Lt. PLIC	Paresis of rt. limbs	None	30	E	D	4	1 day
6/14/M	Rt. frontal	Paresis of lt. limbs, headache	None	111	E	S/D	5	1 day
7/14/M	Rt. frontal	Headache, vomit	2 months	8	N	S	1	4 days
8/16/F	Lt. frontal	Disturbance of consciousness, seizure	None	40	N	S	2	1 day
9/19/F	Lt. temporal	Visual field abnormality, headache	None	46	E	S/D	4	4 days
10/24/M	Lt. parietal	Seizure	None	44	N	S/D	3	1 month
11/27/F	Lt. temporal	None	None	8	N	S	1	3 months
12/35/F	Lt. thalamus	Paresis of rt. limbs	7 months	37	E	D	4	4 days
13/39/F	Rt. temporal	Headache, seizure	3 years	34	N	S/D	3	3 days
14/35/F	Rt. occipital	Headache	1 month	16	E	S/D	3	1 day
15/40/M	Rt. cerebellum	Headache, vomit	14 days	15	N	D	2	3 days
16/47/F	Lt. parietal, temporal	Dizziness	None	53	E	S/D	4	1 day
17/50/M	Lt. parietal	Visual field abnormality, aphasia	None	21	N	D	2	2 days
18/54/M	Rt. frontal	Seizure	None	32	E	S	3	2 days
19/57/M	Midbrain	Headache	9 months	23	E	S/D	3	3 days
20/60/F	Lt. parietal, occipital	Headache	None	62	E	S	4	1 day
21/63/M	Rt. parietal	Seizure	None	24	N	S/D	2	1 day

SM Spetzler-Martin, M male, F female, Rt. right, Lt. left, AVM arteriovenous malformation, DSA digital subtraction angiography, N non-eloquent, E eloquent, S superficial, D deep, PLIC posterior limb of the internal capsule

Table 2 MR imaging parameters

	TOF	AccASL
Acquisition sequence	3D T1-FFE	3D T1-TFE
Acceleration encoding (m/s^2)	None	1.47
TR/TE (ms)	20/3.5	7.5/3.5
Shot interval (ms)	None	1500
Flip angle (deg)	20	11
Turbo factor	None	60
Fat suppression	None	SPIR
Voxel size (mm)	0.39, 0.77, 1.00	0.39, 0.77, 1.00
Slab thickness (mm)	120	120
Number of chunks	4	1
SENSE factor	2.0	2.0
Total scan time	6 min and 9 s	6 min and 9 s

TOF time-of-flight, *AccASL* acceleration-selective arterial spin labeling, *FFE* fast field echo, *TFE* turbo field echo, *TR* repetition time, *TE* echo time, *SPIR* spectral presaturation with inversion recovery, *SENSE* sensitivity encoding

manner. One of the MR angiography (TOF or AccASL) images was displayed on a 20.8-in. liquid crystal display monitor of a picture archiving and communication system. Images other than those from the selected series were not displayed. The observers were allowed to assess raw images, 20-mm-

thick, or full maximum intensity projection (MIP) images of each MR angiography result. The observers were asked to report the presence of the AVM, the size of the nidus, the eloquence of the lesion location, the venous drainage pattern (superficial and/or deep), and the SM grade. The size of nidus was measured on full MIP images of each MR angiography.

Qualitative evaluation of vessel visualization

After the observer study described above, the vessel visualization on the AccASL and TOF was evaluated with a grading scale (Table 3) by the same two neuroradiologists. The DSA image and one of the MR angiography (TOF or AccASL) images from the same patient were concurrently displayed on two monitors. The visualization of the feeding artery, nidus, and draining veins was assessed using the DSA image as the reference standard with a 5-point scale. The visualization of the cortical veins which were not associated with the AVM was also assessed with a 4-point scale.

Quantitative evaluation of vessel visualization

The contrast-to-noise ratio (CNR) was measured in three AVM components by another neuroradiologist (O.T.) with 17 years of experience. First, three to five circular or oval

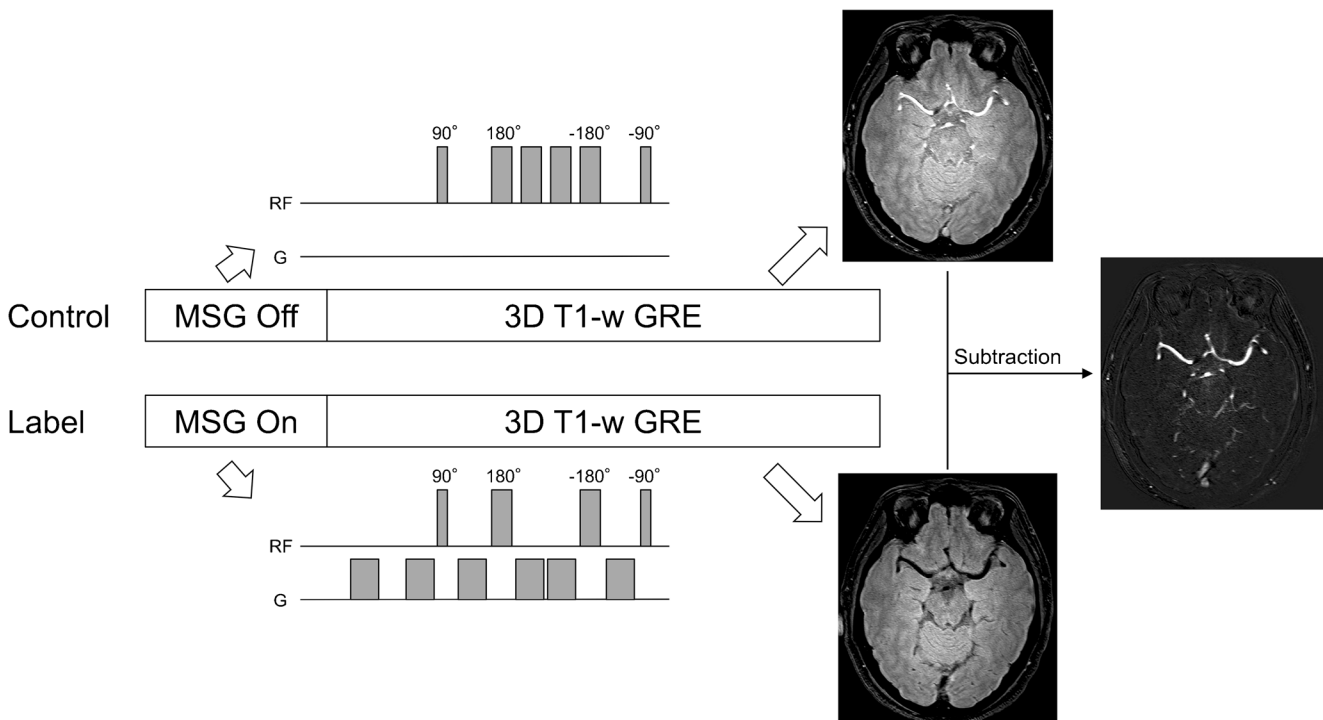


Fig. 2 Schematic overview of the improved version of AccASL (iAccASL). The AccASL sequence consists of a control part and a labeling preparation part followed by a 3D T1-weighted gradient-echo sequence. In the label module, MSGs were applied for a 20-ms period with acceleration encoding such that an acceleration of 1.47 m/s^2 results

in a phase accumulation of exactly π . In the control module, no MSGs were applied, but the two additional 180° refocusing pulses were used to efficiently suppress spin dispersion and flow voids in major arterial trunks. MR angiography is obtained by subtracting the images acquired in labeling from those in the control

Table 3 Criteria for qualitative evaluation of AVM components

Criterion	Interpretation	Scores
Visualization of each component (feeding artery, nidus, and draining vein) in comparison with DSA	Poor, ~25%	1
	Fair, 25~50%	2
	Moderate, 50~75%	3
	Good, 75~90%	4
	Excellent, 90~100	5
Visualization of cortical veins not associated with AVM	No visualization	1
	Large cortical veins are slightly visualized	2
	Large cortical veins are visualized. No visualization of small cortical veins	3
	Most part of cortical veins are visualized	4

AVM arteriovenous malformation, DSA digital subtraction angiography

regions-of-interest (ROIs, typical size 50–70 mm²) were placed on each AVM component (feeding arteries, nidus, or draining veins), as well as on the background stationary tissues (ST) in the brain parenchyma. The same ROI set was used for both the AccASL and TOF images, since both images were obtained in the identical geometry and spatial resolution. The ROIs for feeding arteries or draining veins were placed on a single transverse or sagittal slice at the level of maximum diameter of a nidus. Those ROIs were placed on larger vessels at locations closest to the nidus. The number of ROI depended on the size of the nidus or number of vessels. Basically, when the nidus size was small (<3 cm) or the number of feeding artery or draining vein was one or two, three ROIs were placed. If the nidus size was medium (>3 and <6 cm) or the number of vessel was more than two, four ROIs were placed. If the nidus size was large (>6 cm) or the number of vessel was more than three, five ROIs were placed. Note that multiple measurements were performed on a single vessel in some cases. The observers were allowed to make minor adjustments of the number of ROI. The average value of the measurements in the ROIs was used to represent the patient.

The vessel-to-ST CNRs were calculated using the following equation [12–15]: $CNR = (Vessel_{max} - ST_{ave}) / ST_{SD}$, where $Vessel_{max}$ is the maximum signal intensity in each vessel ROI. The ST_{ave} and ST_{SD} are the mean signal intensity and standard deviation (SD) in the ST ROI, respectively.

Table 4 Kappa statistics for inter-modality agreement between DSA and MR angiography

	Eloquence		Venous drainage pattern		SM grade	
	TOF	AccASL	TOF	AccASL	TOF	AccASL
Observer 1	0.618	0.909	0.480	0.858	0.423	0.878
Observer 2	0.261	0.739	0.190	0.577	0.197	0.617

DSA digital subtraction angiography, TOF time-of-flight, AccASL acceleration-selective arterial spin labeling, SM Spetzler-Martin

DSA findings

Based on the DSA findings, the nidus size, eloquence, venous drainage pattern, and SM grade were determined by the consensus of two board-certified neuroradiologists (O.T., 17 years of experience, A.H., 19 years of experience) who did not participate in the observer study.

Statistical analysis

Inter-modality agreements between DSA and each MR angiography (TOF or AccASL) regarding the eloquence, venous drainage pattern, and SM grade and inter-rater agreements between the two observers were assessed using the kappa statistic (weighted kappa for the degree of agreement) for each observer. Agreement was interpreted based on kappa as follows: ≤0.20, slight; 0.21–0.40, fair; 0.41–0.60, moderate; 0.61–0.80, substantial; and 0.81–1.00, almost perfect. The nidus size was compared among DSA, TOF, and AccASL using a repeated measures analysis of variance (ANOVA) with

Table 5 Kappa statistics for inter-rater agreement between the two observers

	MR angiography	
	TOF	AccASL
Eloquence	0.637	0.831
Venous drainage pattern	0.673	0.724
SM grade	0.697	0.643
Feeding artery score	0.660	0.483
Nidus score	0.468	0.541
Draining vein score	0.689	0.453
Cortical vein score	0.512	1.000

TOF time-of-flight, AccASL acceleration-selective arterial spin labeling, SM Spetzler-Martin

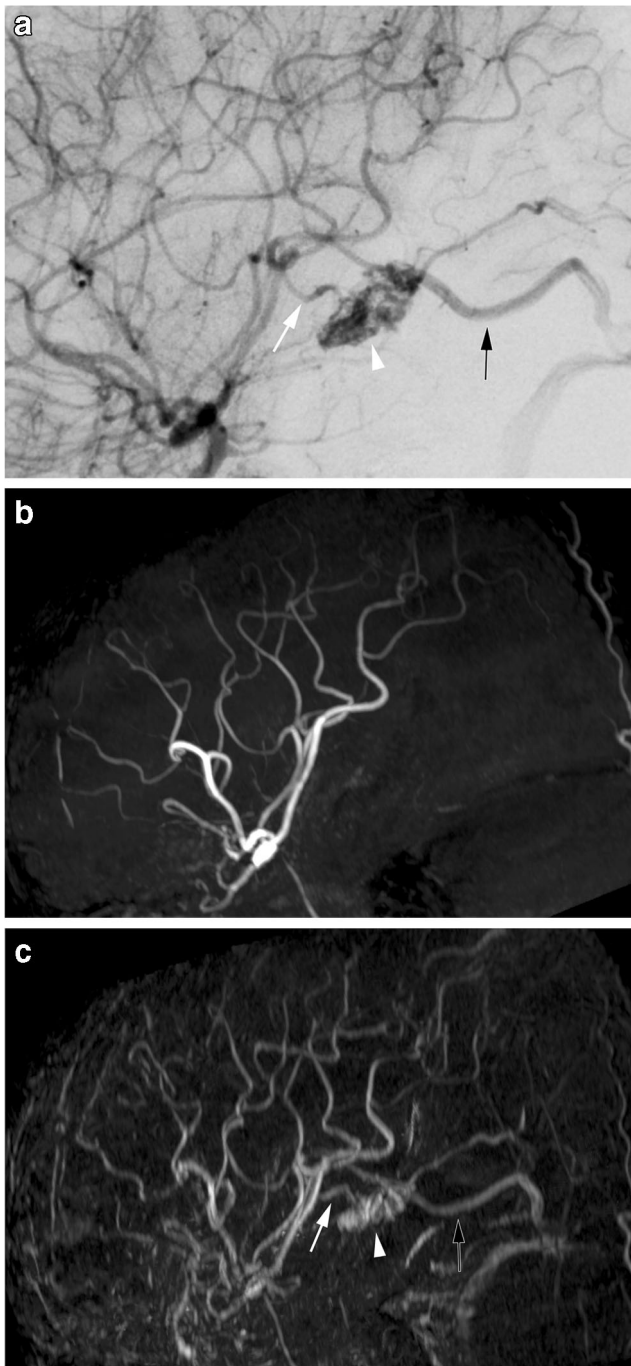


Fig. 3 An 11-year-old male with a brain AVM. The DSA (a) of the right internal carotid artery (ICA) showed the small AVM in the right temporal lobe. The feeding artery (white arrow), nidus (arrowhead), and draining vein (black arrow) were visualized. The sagittal partial maximum intensity projection (MIP) of TOF MR angiography (b) failed to visualize the lesion. The sagittal partial MIP of AccASL MR angiography (c) successfully visualized all three components: the feeding artery (white arrow), nidus (arrowhead), and draining vein (black arrow)

post hoc Tukey's test. The scores for vessel visualization were compared between the two MR methods by the Wilcoxon matched pairs test. The CNRs were compared between the

TOF and AccASL by the paired *t* test. Statistical analyses were performed with Prism 5.0 (GraphPad Software, San Diego, CA) and JMP13 (SAS Institute, Cary, NC). *P* values < 0.05 were considered significant.

Results

Observer study

Both observers detected more AVMs with the AccASL (20 of 21 lesions, 95.2% for Observer 1, 19 of 20 lesions, 90.5% for Observer 2) than with the TOF (Observer 1, 16 of 21 lesions, 76.2%; Observer 2, 15 of 21 lesions, 71.4%) with reference to DSA. A 12-mm AVM in patient no. 4 (Table 1) who had undergone a recent surgery for the hemorrhage from this lesion was not detected on either MR angiography by either observer. The nidus size was not significantly different among DSA (32.1 ± 23.3 mm), TOF (Observer 1, 27.0 ± 25.9 mm; Observer 2, 26.4 ± 20.6 mm), and AccASL (Observer 1, 27.2 ± 23.3 mm; Observer 2, 29.9 ± 20.4 mm) for both observers.

Table 4 shows the kappa statistics for the inter-modality agreement between DSA and each MR angiography for the two observers. The kappa statistics for the eloquence, venous drainage pattern, and SM grade were higher with AccASL than with TOF for both observers. The agreements on the eloquence were moderate and fair on TOF and almost perfect and substantial on AccASL for Observers 1 and 2, respectively. The agreements on the venous drainage pattern were moderate and slight on TOF and almost perfect and moderate on AccASL for Observers 1 and 2, respectively. The agreements on the SM grade were moderate and slight on TOF and almost perfect and substantial on AccASL for Observers 1 and 2, respectively. Table 5 summarizes the kappa statistics for the inter-rater agreement between the two observers. The agreements on the eloquence were substantial on TOF and almost perfect on AccASL. The agreements on the venous drainage pattern and SM grade were substantial on both TOF and AccASL. The agreements on the feeding artery score were substantial on TOF and moderate on AccASL. The agreements on the nidus score were moderate on both TOF and AccASL. The agreements on the draining vein score were substantial on TOF and moderate on AccASL. The agreements for cortical veins score were moderate on TOF and almost perfect on AccASL. Figure 3 shows a case of brain AVM in which TOF failed to detect any components of AVM, whereas the AccASL was able to visualize all components including the nidus and draining veins.

Table 6 Scores for qualitative evaluation

	Feeding artery			Nidus			Draining vein			Cortical veins not associated with AVM		
	TOF	AccASL	<i>P</i>	TOF	AccASL	<i>P</i>	TOF	AccASL	<i>P</i>	TOF	AccASL	<i>P</i>
Observer 1	3.9 ± 1.5	4.5 ± 1.0	0.0214	3.2 ± 1.5	4.6 ± 1.1	0.0006	2.2 ± 1.1	4.6 ± 1.0	<0.0001	1.6 ± 0.7	1.0 ± 0.0	0.0035
Observer 2	3.4 ± 1.7	4.2 ± 1.4	0.00232	2.6 ± 1.2	4.1 ± 1.3	0.0002	2.2 ± 1.1	4.0 ± 1.5	0.0002	1.3 ± 0.5	1.0 ± 0.2	0.0726

TOF time-of-flight, AccASL acceleration-selective arterial spin labeling

Qualitative assessment of vessel visualization

The vessel visualization scores are summarized in Table 6. The scores for both observers were significantly higher with AccASL than with TOF in the visualization of feeding arteries ($p = 0.0214$ and $p = 0.00232$), nidus ($p = 0.0006$ and $p = 0.0002$), and draining veins ($p < 0.0001$ and $p = 0.0002$) for Observers 1 and 2, respectively. The cortical vein scores were significantly higher with TOF than with AccASL for Observer 1 ($p = 0.0035$), whereas they were not significantly different between the methods for Observer 2 ($p = 0.0726$).

Figure 4 shows a representative case of brain AVM in which the AccASL better visualized all components especially for the nidus and draining veins. Figure 5 shows a case of large AVM of SM grade 5. The TOF failed to depict the deep draining veins (which led to the underestimation of SM grade), whereas the AccASL successfully visualized these veins and thus enabled accurate grading. Figure 6 shows a case of ruptured AVM: the AVM was better depicted on AccASL than on TOF since the signal from the hematoma with a T1-shortening effect was suppressed due to subtraction in AccASL.

Quantitative evaluation of vessel visualization

The CNRs in each component across all patients are illustrated in Fig. 7. The CNRs in the feeding arteries (TOF, 37.5 ± 28.6 ; AccASL, 31.0 ± 15.7 , $p = 0.2171$) were not significantly different between the TOF and AccASL. The CNRs in the nidus (TOF, 20.8 ± 16.5 ; AccASL, 29.9 ± 16.7 , $p = 0.0002$) and draining veins (TOF, 12.6 ± 12.0 ; AccASL, 23.2 ± 13.0 , $p = 0.0010$) were significantly higher with the AccASL than with the TOF.

Discussion

Our findings demonstrated the clinical potential of AccASL in visualizing complex or slow flows and flows that are not in the

inferior-to-superior direction in brain AVMs, which are typical limitations of TOF.

The observer study revealed that AccASL provided better AVM detection than TOF, and it showed that the inter-modality agreement of AccASL with DSA as the reference standard was good (from moderate to almost perfect) in the evaluation of the eloquence, venous drainage pattern, and SM grade without reference to any other clinical images. TOF has been used clinically for the evaluation of brain AVMs, but its application has remained of supplementary support because of its lack of consistent and complete demonstrations of all components of AVMs [5, 16–18]. Because of the limitations mentioned above, TOF is not always adequate for the assessment of morphological features of AVM such as the size and extent of the nidus, the eloquence of the lesion location, and the deep venous drainage, which are of great importance since they can affect the therapeutic strategy and have prognostic implications. AccASL can be suitable for such morphological assessments of brain AVMs.

Inter-modality agreements between DSA and MR angiography were higher in Observer 1 than in Observer 2 on both methods and were higher on AccASL than on TOF for both observers. The improvements in the agreements from TOF to AccASL were more prominent in Observer 2. This was probably due to the less experience of Observer 2; Observer 1 had 15 years of experience in neuroradiology while Observer 2 had only 4 years. Inter-rater agreements were moderate or substantial (kappa statistics > 0.4) for all items on both TOF and AccASL, which assures the reliability of the measurements by the two observers in spite of the difference in their experience.

Our qualitative and quantitative evaluations revealed that the visualization scores and CNRs with TOF decreased from feeding arteries to the nidus and from the nidus to draining veins, presumably reflecting a gradual reduction of inflow effect and flow velocity within an AVM. On the other hand, AccASL retained high visualization scores even in the nidus and draining veins. The CNR reduction from feeding arteries to draining veins on AccASL (25%) was much smaller than on that on TOF (67%). As a result, AccASL better depicted all components of AVMs compared to TOF, and the scores obtained with AccASL compared to DSA were excellent in the majority of cases. These results indicated that the AccASL

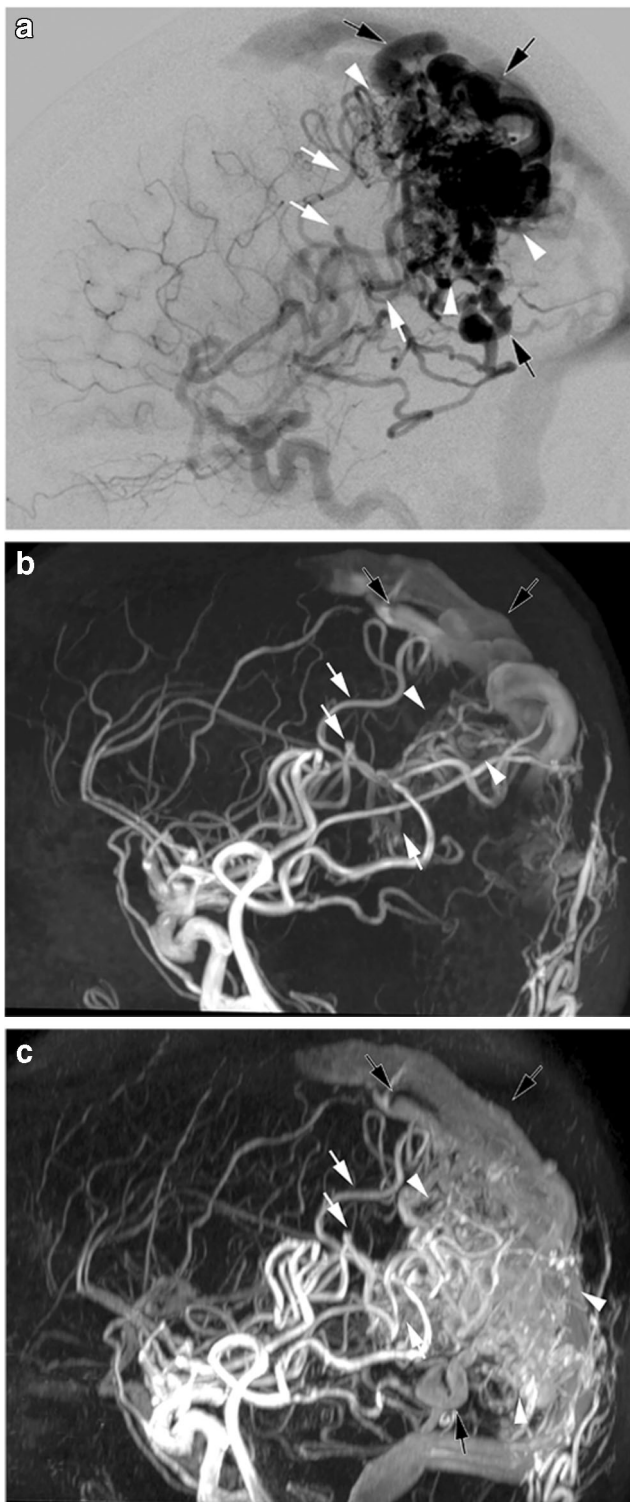


Fig. 4 A 60-year-old female with a brain AVM. The DSA (a) of the left ICA showed the large AVM in the left parietal and occipital lobes. The feeding arteries (*white arrows*), nidus (*arrowheads*), and draining veins (*black arrows*) were visualized. The sagittal MIP of TOF (b) showed the good visualization of feeding arteries (*white arrows*) but reduced visualization of the nidus (*arrowheads*) and draining veins (*black arrows*). The sagittal MIP of AccASL (c) showed the good visualization of feeding arteries (*white arrows*), nidus (*arrowheads*), and draining veins (*black arrows*)

◀ **Fig. 5** A 14-year-old male with a brain AVM. The dyna-CT angiography (a) of the right ICA showed the large AVM in the right frontal lobe. The deep draining veins (black arrows) were visualized. The axial MIP of TOF (b) failed to visualize these veins. The axial MIP of AccASL (c) successfully visualized these deep draining veins (black arrows), which allowed for the accurate SM grading

was sensitive enough to identify complex flows in the nidus and slow flows in draining veins. In general, the vessels with a higher CNR in TOF showed a reduced CNR in AccASL, whereas the vessels with a lower CNR in TOF showed an increased CNR in AccASL. This trend was also observed in a prior study on moyamoya disease [10]. This indicates that AccASL is not good at the visualization of vessels with relatively fast flow. Additionally, AccASL is very sensitive to patient's motion since this technique is based on the subtraction of two image sets. When considering these issues, it is likely that AccASL works as a supportive tool which should be added to TOF at this moment. In other words, both methods act in a mutually beneficial manner in visualizing vessel diseases. Further development of AccASL, specifically for better visualizations of proximal arteries and reduction of motion artifacts, is desired before it could replace TOF.

The delineation of AVM on TOF is frequently limited by high signal due to a T1-shortening effect in a subacute hemorrhage from a ruptured AVM. AccASL would be expected to better depict AVMs since such a high signal in a hemorrhage is cancelled out due to the subtraction of the images acquired in labeling from those in the control. In fact, a ruptured AVM was not detected on TOF by either of the present study's observers because of a subacute hemorrhage, although the ruptured AVM was successfully detected on AccASL by both observers.

Our results also revealed that no normal cortical veins were identified by the visual assessment in most of the patients, which indicates the effectiveness of the acceleration-sensitive design of the AccASL sequence. This was consistent with another study of adult volunteers [9]. In TOF, the suppression of the cortical vein signal is insufficient in the uppermost slab since the spatial saturation to suppress the vein signal is difficult. The suppression of signal from normal cortical veins is very important for the selective visualization of draining veins of an AVM. Contrast-enhanced MR angiography would increase signal and reduce the saturation effect in the nidus and draining veins, but the veins that are not associated with AVM would be visualized, which makes it difficult to selectively visualize draining veins. However, signals due to a relatively fast flow in large dural venous sinuses remain in normal subjects on AccASL, which can compromise the understanding of venous outflow in AVMs.

Contrast-enhanced MR angiography could overcome some of the aforementioned problems of the saturation effect in TOF. Dural et al. reported that TOF MR angiography could

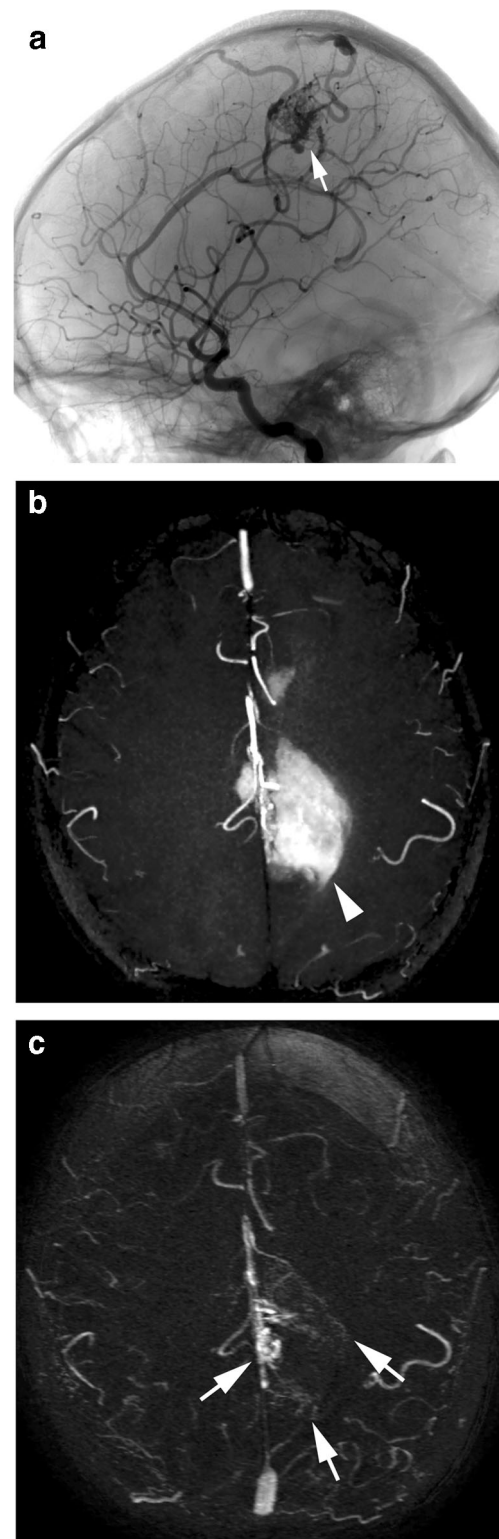


Fig. 6 An 11-year-old male with a ruptured brain AVM and subacute hematoma. The DSA (a) of the left ICA showed the small nidus (arrow) in the left parietal lobe. The axial partial MIP of TOF (b) showed poor delineation of the nidus because of the high signal due to the T1-shortening effect in the adjacent subacute hematoma (arrowhead). The axial MIP of AccASL (c) showed the good visualization of the nidus (arrows) since the signal in the hematoma was cancelled out due to the subtraction of the images acquired in labeling from those in the control

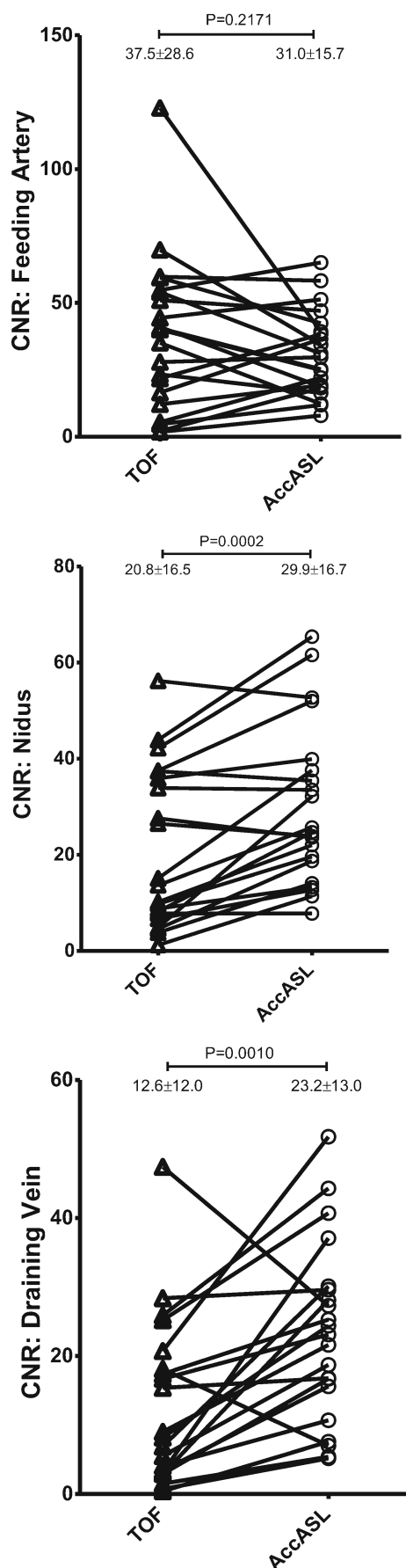


Fig. 7 The CNR in each component across all patients. The CNRs in the feeding arteries (TOF, 37.5 ± 28.6 ; AccASL, 31.0 ± 15.7 , $p = 0.2171$) were not significantly different between the TOF and AccASL. The CNRs in the nidus (TOF, 20.8 ± 16.5 ; AccASL, 29.9 ± 16.7 , $p = 0.0002$) and draining veins (TOF, 12.6 ± 12.0 ; AccASL, 23.2 ± 13.0 , $p = 0.0010$) were significantly higher with the AccASL than with the TOF

demonstrate the exact venous drainage in only 9 of 22 patients, whereas contrast-enhanced MR angiography clearly delineated it in most of the patients [19]. Griffiths et al. reported that with the use of contrast-enhanced 4D MR angiography, the nidus of the AVM was depicted in 19 of 20 patients, and venous drainage was correctly assessed in 18 of 19 cases. However, the spatial resolution in contrast-enhanced 4D MR angiography can be limited since temporal information takes a priority over spatial resolution. Although AccASL has no temporal information, high spatial resolution identical to that of TOF would help for a delineation of fine vascular anatomy.

Several studies indicated that spatially selective 3D or 4D arterial spin labeling (ASL) could be useful for intracranial MR angiography in the visualization of slow, in-plane, or complex flows in AVMs [15, 20, 21]. However, the vessel signal in spatially selective ASL largely depends on the transit time from the labeling region to the targeted region. Thus, these methods could be of limited utility for visualizing very slow flows in draining veins, in which the transit time could be longer than the T1 of the blood (1.6 s at 3 T). Additionally, the spatial resolution in spatially selective 4D ASL MR angiography is limited.

Our study has limitations. First, we did not compare AccASL with contrast-enhanced MR angiography, spatially selective ASL MR angiography, or CT angiography since these images were not obtained in all patients. Second, AccASL as in any other arterial spin labeling approaches is sensitive to patient movement. Although severe motion artifact was not observed in this patient series, subtle motion could have reduced the signal in vessels. The use of motion compensation with post-processing should be considered for future clinical trials. Finally, we could not minimize the bias regarding the identification of the MR angiography methods, and it was easy for the observers to identify the type of MR angiography. Instead, to minimize the possible influence from the other type of MR angiography, both observers took part in two reading sessions ≥ 1 month apart, and images other than those from the selected series were not displayed.

In conclusion, AccASL MR angiography provided better visualization of all components in brain AVMs and higher performance in assessing SM grade compared with conventional TOF MR angiography. AccASL could serve as a non-invasive tool to evaluate AVMs without the use of contrast agents or radiation. The observations of lesions by AccASL might be useful when selecting the therapeutic strategy and monitoring after treatment in patients with brain AVMs.

Acknowledgements The authors would like to thank Dr. Yukiko N. Kami for useful discussions on the statistical analyses.

Compliance with ethical standards

Conflict of interest MO and MVC are employees of Philips Japan.

Ethical approval All procedures performed in the studies involving human participants were in accordance with the ethical standards of the institutional research committee and with the 1964 Helsinki Declaration and its later amendments or comparable ethical standards.

Informed consent Informed consent was waived due to the retrospective nature of this study.

References

- Hernesniemi JA, Dashti R, Juvela S, Vaart K, Niemela M, Laakso A (2008) Natural history of brain arteriovenous malformations: a long-term follow-up study of risk of hemorrhage in 238 patients. *Neurosurgery* 63(5):823–829; **discussion 829–831**. <https://doi.org/10.1227/01.NEU.0000330401.82582.5E>
- Laakso A, Dashti R, Juvela S, Isarakul P, Niemela M, Hernesniemi J (2011) Risk of hemorrhage in patients with untreated Spetzler-Martin grade IV and V arteriovenous malformations: a long-term follow-up study in 63 patients. *Neurosurgery* 68(2):372–377; **discussion 378**. <https://doi.org/10.1227/NEU.0b013e3181ffe931>
- Morgan MK, Davidson AS, Assaad NNA, Stoodley MA (2017) Critical review of brain AVM surgery, surgical results and natural history in 2017. *Acta Neurochir* 159(8):1457–1478. <https://doi.org/10.1007/s00701-017-3217-x>
- Marchal G, Bosmans H, Van Fraeyenhoven L, Wilms G, Van Hecke P, Plets C, Baert AL (1990) Intracranial vascular lesions: optimization and clinical evaluation of three-dimensional time-of-flight MR angiography. *Radiology* 175(2):443–448. <https://doi.org/10.1148/radiology.175.2.2326471>
- Wilcock DJ, Jaspan T, Worthington BS (1995) Problems and pitfalls of 3-D TOF magnetic resonance angiography of the intracranial circulation. *Clin Radiol* 50(8):526–532
- Huston J 3rd, Rufenacht DA, Ehman RL, Wiebers DO (1991) Intracranial aneurysms and vascular malformations: comparison of time-of-flight and phase-contrast MR angiography. *Radiology* 181(3):721–730. <https://doi.org/10.1148/radiology.181.3.1947088>
- Priest AN, Taviani V, Graves MJ, Lomas DJ (2014) Improved artery-vein separation with acceleration-dependent preparation for non-contrast-enhanced magnetic resonance angiography. *Magn Reson Med* 72(3):699–706. <https://doi.org/10.1002/mrm.24981>
- Schmid S, Ghariq E, Teeuwisse WM, Webb A, van Osch MJ (2014) Acceleration-selective arterial spin labeling. *Magn Reson Med* 71(1):191–199. <https://doi.org/10.1002/mrm.24650>
- Obara M, Togao O, Yoneyama M, Okuaki T, Shibukawa S, Honda H, Van Cauteren M (2016) Acceleration-selective arterial spin labeling for intracranial MR angiography with improved visualization of cortical arteries and suppression of cortical veins. *Magn Reson Med* 77:1996–2004. <https://doi.org/10.1002/mrm.26275>
- Togao O, Hiwatashi A, Obara M, Yamashita K, Kikuchi K, Kamei R, Nishimura A, Arimura K, Yoshimoto K, Iihara K, Van Cauteren M, Honda H (2017) Acceleration-selective arterial spin-labeling MR angiography used to visualize distal cerebral arteries and collateral vessels in moyamoya disease. *Radiology*:162279 286: 611–621. <https://doi.org/10.1148/radiol.2017162279>
- Akamine Y, Obara M, Togao O, Shibukawa S, Yoneyama M, Okuaki T, Van Cauteren M (2017) Robust visualization of MCA main trunk by improved acceleration-selective arterial spin labeling (iAccASL) for intracranial MR angiography. *Proc Int Soc Magn Reson Med* 25:361
- Obara M, Togao O, Yoneyama M, Okuaki T, Shibukawa S, Honda H, Van Cauteren M (2017) Acceleration-selective arterial spin labeling for intracranial MR angiography with improved visualization of cortical arteries and suppression of cortical veins. *Magn Reson Med* 77(5):1996–2004. <https://doi.org/10.1002/mrm.26275>
- Togao O, Hiwatashi A, Obara M, Yamashita K, Kikuchi K, Kamei R, Nishimura A, Arimura K, Yoshimoto K, Iihara K, Van Cauteren M, Honda H (2018) Acceleration-selective arterial spin-labeling MR angiography used to visualize distal cerebral arteries and collateral vessels in moyamoya disease. *Radiology* 286(2):611–621. <https://doi.org/10.1148/radiol.2017162279>
- Tsuchiya K, Kobayashi K, Nitatori T, Kimura T, Ikedo M, Takemoto S (2010) Hybrid of opposite-contrast MRA of the brain by combining time-of-flight and black-blood sequences: initial experience in major trunk stenooclusive diseases. *J Magn Reson Imaging* 31(1):56–60. <https://doi.org/10.1002/jmri.21997>
- Wu H, Block WF, Turski PA, Mistretta CA, Johnson KM (2013) Noncontrast-enhanced three-dimensional (3D) intracranial MR angiography using pseudocontinuous arterial spin labeling and accelerated 3D radial acquisition. *Magn Reson Med* 69(3):708–715. <https://doi.org/10.1002/mrm.24298>
- Kauczor HU, Engenhart R, Layer G, Gamroth AH, Wowra B, Schad LR, Semmler W, van Kaick G (1993) 3D TOF MR angiography of cerebral arteriovenous malformations after radiosurgery. *J Comput Assist Tomogr* 17(2):184–190
- Ehrlicke HH, Schad LR, Gademann G, Wowra B, Engenhart R, Lorenz WJ (1992) Use of MR angiography for stereotactic planning. *J Comput Assist Tomogr* 16(1):35–40
- Blatter DD, Parker DL, Ahn SS, Bahr AL, Robison RO, Schwartz RB, Jolesz FA, Boyer RS (1992) Cerebral MR angiography with multiple overlapping thin slab acquisition. Part II. Early clinical experience. *Radiology* 183(2):379–389. <https://doi.org/10.1148/radiology.183.2.1561338>
- Duran M, Schoenberg SO, Yuh WT, Knopp MV, van Kaick G, Essig M (2002) Cerebral arteriovenous malformations: morphologic evaluation by ultrashort 3D gadolinium-enhanced MR angiography. *Eur Radiol* 12(12):2957–2964. <https://doi.org/10.1007/s00330-002-1418-y>
- Fujima N, Osanai T, Shimizu Y, Yoshida A, Harada T, Nakayama N, Kudo K, Houkin K, Shirato H (2016) Utility of noncontrast-enhanced time-resolved four-dimensional MR angiography with a vessel-selective technique for intracranial arteriovenous malformations. *J Magn Reson Imaging* 44(4):834–845. <https://doi.org/10.1002/jmri.25222>
- Raoult H, Bannier E, Robert B, Barillot C, Schmitt P, Gauvrit JY (2014) Time-resolved spin-labeled MR angiography for the depiction of cerebral arteriovenous malformations: a comparison of techniques. *Radiology* 271(2):524–533. <https://doi.org/10.1148/radiol.13131252>

Publisher's note Springer Nature remains neutral with regard to jurisdictional claims in published maps and institutional affiliations.